AN OPTIMAL VOTING SCHEME FOR MICROANEURYSM CANDIDATE EXTRACTORS USING SIMULATED ANNEALING

Bálint Antal, István Lázár and András Hajdu
University of Debrecen, Faculty of Informatics, POB 12, 4010 Debrecen, Hungary

Keywords: Biomedical image processing, Image classification, Pattern recognition, Medical decision-making, Statistics.

Abstract: In this paper, we present a novel approach to improve microaneurysm candidate extraction in color fundus images. The individual algorithms published so far can be hardly considered in an automatic screening system. To improve further the sensitivity, specificity and image classification rate of microaneurysm detection, we propose an appropriate combination of individual algorithms. Thus, we investigate the detection of microaneurysms through the following phases: first, we use different approaches to extract microaneurysm candidates. Then, we select candidates voted by a sufficient number of the candidate extractor algorithms. The optimal number of votes and participating algorithms are determined by a simulated annealing algorithm. Finally, we classify the candidates with a machine-learning based approach by following the current literature recommendations. Our framework improves the positive likelihood ratio for the microaneurysms and outperforms both the state-of-the-art individual candidate extractors and microaneurysm detectors in these terms.

1 INTRODUCTION

Diabetic retinopathy (DR) is the most common cause of blindness in the developed countries. Microaneurysms (MAs) are early signs of this disease, so the detection of these lesions is essential in the screening process. DR can be prevented and its progression can be slowed down if diagnosed and treated early. A proper medical protocol (Harding et al., 2003), (Committee, 2009) has been established, but the actual grading required for diagnostics has been performed manually. Manual grading is slow and resource demanding, so several efforts have been made to establish an automatic computer-aided screening system (Abramoff et al., 2008), (Hejlesen et al., 2004). However, the detection of microaneurysms is still an open issue. Thus, several recent works focus on this problem, including an online challenge for MA detectors (Niemeijer et al., 2010).

Microaneurysms appear as small circular dark spots on the surface of the retina (see Figure 1). The most common appearance of microaneurysms is near thin vessels, but they cannot actually lie on the vessels. In some cases, microaneurysms are hard to distinguish from parts of the vessel system. For example, the intersections of two thick vessels or a few very thin vessels are rather misleading for the detectors.

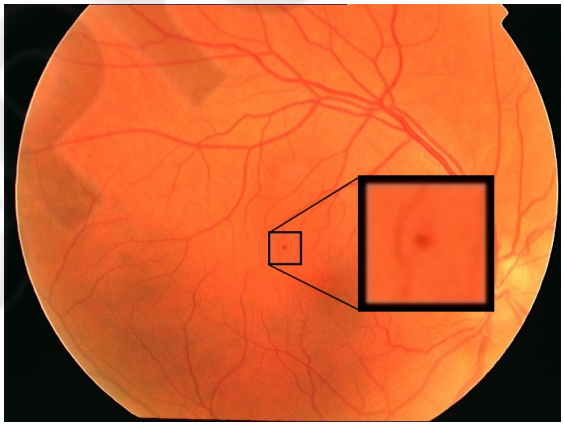

Figure 1: Fundus image containing a microaneurysm.

In this paper, we propose an ensemble-based approach to MA detection to suppress the errors of individual algorithms. The proposed process consists of three main steps (see also Figure 2): first, we extract MA candidates from fundus images after preprocessing. For this task, we select three state-of-the-art approaches and include a novel one, as well. In the second phase, we combine the results provided by the four candidate extractors and reduce the number of candidates with a voting scheme. The number of required votes and the set of the corresponding candidate extractors is determined by a simulated annealing algorithm. We also introduce a novel machine-learn-

Antal B., Lázár I. and Hajdu A. (2010).
AN OPTIMAL VOTING SCHEME FOR MICROANEURYSM CANDIDATE EXTRACTORS USING SIMULATED ANNEALING.
In *Proceedings of the International Conference on Signal Processing and Multimedia Applications*, pages 80-87

ing based algorithm to classify the candidates. The rest of the paper is organized as follows. In section 2 we present the MA candidate extractor algorithms to build up an ensemble. The optimal voting scheme of the MA extractor algorithms is described in section 3. In section 4 the results of the ensemble-based system are presented. Finally, some conclusions are drawn in section 5.

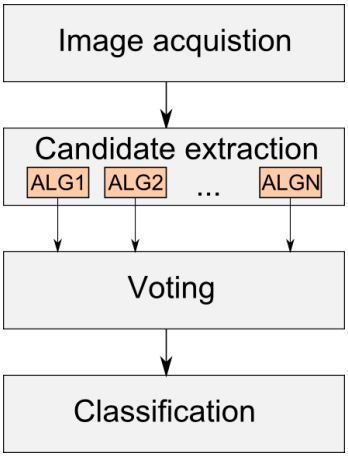

Figure 2: Steps of microaneurysm detection using an ensemble of candidate extractors.

2 MICROANEURYSM CANDIDATE EXTRACTION

Candidate extraction is an effort to reduce the number of objects in an image for further analysis by excluding regions which do not have similar characteristics to microaneurysms. Individual approaches define their own measurement for similarity to extract MA candidates. In this section, we provide a brief overview of currently popular candidate extractors that will be considered later on in the ensemble system. Namely, we recall Walter et al. (Walter et al., 2007), the Spencer-Frame method (Spencer et al., 1996) (Frame et al., 1998) in its original form, and a slightly modified version of (Abdelazeem, 2002). A new approach is also involved, whose development was partly motivated to improve the MA candidate extraction efficiency of the proposed ensemble-based system. As we will see later on, these methods sufficiently diverse to form a successful ensemble.

2.1 Walter et al.

This approach is proposed in (Walter et al., 2007). To overcome the imperfections of color fundus images, a contrast enhancement operator is applied as a preprocessing step along with shade correction:

$$[SC(f)] = \begin{cases} \frac{\frac{1}{2}(u_{max}-u_{min})\cdot(f(x)-t_{min})^r}{\left(\mu_f^*-t_{min}\right)^r} + u_{min}, & t \leq \mu_f^* \\ \frac{-\frac{1}{2}(u_{max}-u_{min})\cdot(f(x)-t_{max})^r}{\left(\mu_f^*-t_{max}\right)^r} + u_{max}, & t \geq \mu_f^* \end{cases}$$

where $\{t_{min}, \ldots t_{max}\}$ are the intensity values of the grayscale image, $\{u_{min}, \ldots u_{max}\}$ are the intensity values of the enhanced image, μ_f^* is the mean value of an area opened image and $r \in \mathbb{R}$. The parameter r controls the level of contrast enhancement. Candidate extraction is then accomplished by grayscale diameter closing. That is, the method aims find all sufficiently small dark patterns on the green channel. Let

$$\alpha(X) = \max_{x,y \in X} d(x,y)$$

be the diameter α of a connected set X with a distance function $d(.)$. Let

$$X_t^-(f) = \{x | f(x) \leq t\}.$$

Then, the grayscale diameter closing is defined by the following formula:

$$\phi_\alpha^o = \inf\{s \geq f(x) \,|\, \alpha\left(C_x\left[X_s^-(f)\right]\right) \geq \alpha\}.$$

Then, the candidates are the remaining objects on the image. For an example output, see Figure 3.

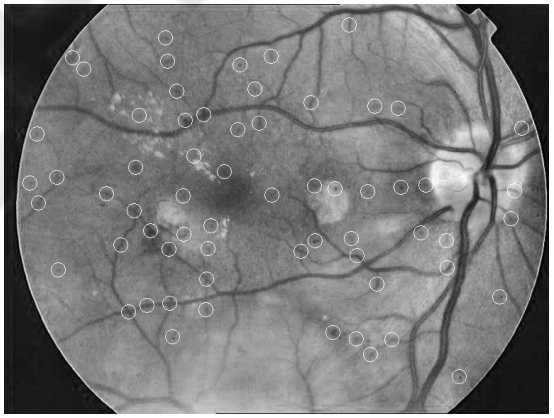

Figure 3: Candidates extracted by the Walter candidate extractor.

2.2 Spencer-Frame

This approach is one of the most popular candidate extractors, originally proposed by (Spencer et al., 1996) and (Frame et al., 1998). The algorithm uses shade correction as preprocessing: first, a background image i_{bg} is produced by applying a median filter on the green channel of the original image i_{green}. Then,

the shade corrected image i_{sc} is established by the following formula:

$$i_{sc} = i_{bg} - i_{green}.$$

The actual candidate extraction is accomplished by subtracting the maximum of multiple morphological top-hat transformations, which is defined as follows:

$$T(f) = f \bullet s - f,$$

where $\bullet$ denotes the morphological closing. For this step, twelve rotated structuring elements were used with a radial resolution of 15°. Then, the vascular map is subtracted from i_{sc} to remove the largest components form the image. As a contras enhancement operator, a 2D Gaussian matched filter is applied on the image. The resulting image is then binarized with a fixed threshold. Since the candidates are not a good representation for the actual lesions, a region growing step is also applied.

A slightly modificated version of this method is proposed in (Niemeijer et al., 2005), (Mizutani et al., 2009) and (Fleming et al., 2006).

For an example output, see Figure 4.

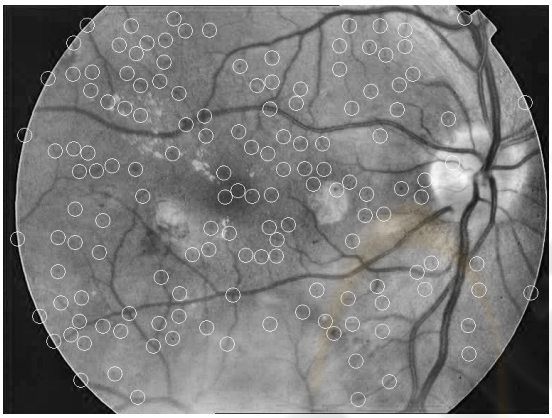

Figure 4: Candidates extracted by the Spencer-Frame candidate extractor.

2.3 Circular Hough-transformation based

Based on the idea presented in (Abdelazeem, 2002), we established an approach based on the detection of small circular spots in the image. As a preprocessing step, a common biomedical image correction technique, the contrast limited adaptive histogram equalization (CLAHE) is applied (Zuiderveld, 1994). CLAHE is realized in the following way (Reza, 2004): first, the image is divided into disjoint regions. Then, for each region a histogram and a clipping limit are obtained. After that, all the histograms are redistributed according to the corresponding limit. Finally, the cumulative distribution functions are determined for grayscale mapping. The candidate extraction is obtained by detecting circles on the images. For this purpose we use circular Hough transformation (Chen and Chung, 2001). With this technique, a set of approximately circle-shaped objects can be obtained from the image. The radius of the circles are limited according to the observed size of microaneurysms from a training set.

For an example output, see Figure 5.

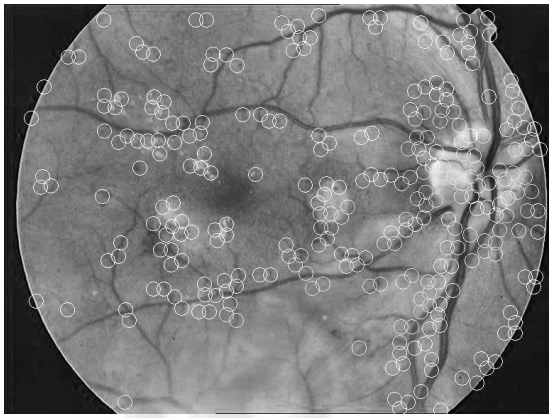

Figure 5: Candidates extracted by the Circular Hough-transformation based candidate extractor.

2.4 Lazar et al.

Besides some popular techniques mentioned so far, we also investigate a new MA candidate extractor developed by our research group.

The green channel of the image is inverted and smoothened with a Gaussian filter. A set of scan lines with equidistantly sampled tangents between -90° and +90° is fixed. For each direction the intensity values along the scan lines are recorded in a one dimensional array, and the scan lines are shifted vertically and horizontally to process every image pixel of the image. On each intensity profile, the heights of the peaks, and their local maximum positions are used for an adaptive thresholding. The resulting foreground indices of the thresholding process are transformed back to two dimensional coordinates, and stored in a map that records the number of foreground pixels of different directions corresponding to every position of the image. The maximal value for each position equals the number of different directions used for the scanning process. This map is smoothened with an averaging kernel and a hysteresis thresholding procedure is applied. The resulting components are filtered based on their size. For more details, see (Lazar et al., 2010).

For an example output, see Figure 6.

Figure 6: Candidates extracted by the Lazar candidate extractor.

2.5 Diversity of the Candidate Extractors

It is important to use diverse candidate extractors, that is, to reduce the number of false positives efficiently and keep only those candidates on which multiple methods agree. As the most straightforward measure, we aim to raise the the positive likelihood ratio (number of the true positive (TP) / number of the false positive (FP)) (Johnson, 2004) using an ensemble.

The pairwise diversity of the classifiers can be measured by the disagreement (D) and double fault (DF) measure, where D, DF $\in [0, 1]$. The disagreement measure sums the cases, where the extractors disagree, but one of them is correct. The double fault measure is the number of candidates, where both extractors agree and both are incorrect. For our aims, a high disagreement and a low double fault measure is the ideal. As it can be seen in Table 1, the selected candidate extractors are quite diverse.

Table 1: Diversity of the candidate extractors.

Walter	Spencer	Hough	Lazar	D	DF
x	x			0.73	0.09
x		x		0.77	0.04
x			x	0.49	0.10
	x	x		0.79	0.06
	x		x	0.69	0.14
		x	x	0.74	0.12

3 AN OPTIMAL VOTING SCHEME FOR COMBINING THE CANDIDATE EXTRACTORS

In this chapter, we present a new approach to select the optimal combination of the candidate extractors. First, for the proper comparison of the candidates extracted by the individual approaches, we must preprocess them. Then, we select an optimal configuration for the voting scheme by a simulated annealing algorithm. Finally, the voting is executed using this configuration. Later on, we present some properties of this optimal voting scheme.

3.1 Preprocessing the Candidates

Before letting the individual candidate extractor algorithms vote, we must ensure that there are no candidates too close to each other within the output of an individual algorithm. This issue is addressed by merging them. It is also important to remove any candidates falling on the vessel system. For this purpose, we have detected the vascular system with the algorithm proposed in (Staal et al., 2004) and removed the candidates falling on vessels.

3.2 Selecting an Optimal Voting Configuration using Simulated Annealing

The proposed framework aims to find an optimal voting scheme for candidate extractors. This voting scheme determines a subset of the candidate extractors and the number of required votes. Since this problem induces a large search space, we use simulated annealing to find an optimal solution.

Simulated annealing (Kirkpatrick et al., 1983) is a widely used global optimization method. This approach is inspired by the annealing in metallurgy. It is effective for large search space problems by using random sampling to avoid stuck in a local minimum. For the optimization, we use the following energy function to be minimized:

$$E = -\frac{TP}{FP},$$

where TP stands for the number of the true, while FP stands for that of the false positive candidates, respectively.

To minimize the target energy E by simulated annealing, each element of the search space S consists of the results sets of a set of candidate extrac-

tors $\{ce_1, \ldots ce_L\}$ and a required number of votes v ($1 \leq v \leq L$). Each combination occurs in S only once.

The proposed simulated annealing algorithm operates through the following steps:

1. Let T be an initial temperature, T_{min} a minimal temperature, $0 \leq q \leq 1, q \in \mathbb{R}$ the temperature change, $S = P((\{R_{ce}\}, v))$ the search space, where R_{ce} is the result of the candidate extractor ce, v is the number of required votes and $P(X)$ is the power set of X.
2. Choose $x \in S$ randomly and let $e = E(x)$, $S = S - \{x\}$.
3. Choose $x_i \in S$ randomly and let $e_i = E(x_i)$, $S = S - \{x_i\}$.
4. If $T < T_{min}$ or $S = \emptyset$, then stop.
5. If $e_i < e$, then $x = x_i$, $e = e_i$ and $T = T \cdot q$. Go to step 4.
6. Choose a random number $r \in \mathbb{R}$. If $accept(e, e_i, T, r) = true$, then $x = x_i$, $e = e_i$, where
$$accept(e, e_i, T, r) = \begin{cases} true, & if \exp\left(\frac{e-e_i}{T}\right) > r, \\ false, & otherwise. \end{cases}$$
7. Let $T = T \cdot q$. Go to step 4.

Currently, we consider four candidate extractors (that is, $L = 4$ in the algorithm above), but with the use of simulated annealing it can be easily extended to more methods in the future.

3.3 Voting on the Candidates

Each individual candidate extractor algorithm produces an initial set of microaneurysm candidates. Then, we establish a set of final candidates, where these candidates are voted by at least $n \geq 2$ candidate extractors. The voting procedure has the following steps:

1. For each candidate c provided by one of the algorithms, check, whether there is another candidate detected by another algorithm within a distance $r \in \mathbb{R}$ from c.
2. Let *sum* be the number of candidates satisfying the above proximity criterion and remove all these candidates from their respective initial sets.
3. If $sum \geq n$, then add the centroid of the candidates found by step 2 to the final set.
4. Repeat the procedure until all the initial sets become empty.

The result of the voting for the previously shown example is presented in Figure 7.

Figure 7: Result of the voting.

3.4 Properties of the Optimal Voting Scheme

Property 1. *The optimal voting scheme selects a subset of the candidate extractors.*

That is, it is not mandatory that all available candidate extractors participate in the voting.

Property 2. *An individually less accurate algorithm can be still useful in an ensemble.*

The optimal voting scheme can make use of some individually less accurate algorithm in certain situations. The results of a simple majority voting with a fixed configuration can be less accurate with a weaker participant.

Property 3. *The use of simulated annealing makes it possible to include a large number of candidate extractors.*

The number of combinations using n candidate extractors is $2^n - 1$ with excluding the empty combination. For a large search space, an approximately optimal solution can also be obtained with simulated annealing by setting a proper annealing schedule in less computational time.

Property 4. *The optimal voting scheme determines the number of required votes from the candidate extractors.*

Thus, the system is more flexible when changing energy functions.

3.5 Candidate Classification

To improve the TP / FP ratio we use a consequent classification step, which is based on certain unique features of microaneurysms. We use a new approach

to perform this step, instead of other literature recommendations. The reason to introduce a new classifier is that the existing methods use objects and not single pixels representations to extract features, while our ensemble-based system provides the latter.

Candidates are classified as actual MAs or non-MAs in two steps. First, we train our approach with several fixed size (e.g. 21×21 pixels) subimages for both microaneurysm and random non-microaneurysm examples. Then, for each pixel of the examples, we establish a kernel density estimator for both classes. After the training step, we can classify new instances. We establish a new instance by producing a subimage of the candidate pixel and its neighborhood with the same size as the training step. The classification procedure is then the following: for each pixel of the instance we compare the probability provided by the kernel density estimators for both classes. Then, the candidate is considered as a microaneurysm if more comparisons confirm that this is a positive example. For the stages of our classifier, see Figure 8.

Formally, the classifier can be described in the following way:

Let

$$E = \{I_1, I_2, \dots I_m\}$$

an ensemble of classifiers, where

$$I : x \to C, x \in D \subset \mathbb{R}^+$$

and C is a class. In our case,

$$D = \{0, 1, \dots 255\}$$

and

$$C \in \{C_{MA}, C_{Non-MA}\},$$

where C_{MA} and C_{Non-MA} denotes the class of Microaneurysms and Non-Microaneurysms, respectively. Let

$$T = \{\langle X_1, c_1\rangle, \langle X_2, c_2\rangle, \dots \langle X_m, c_m\rangle\}$$

be the training dataset, where

$$X_j = \{x_{j1}, x_{j2}, \dots x_{jn},\},$$

$$x_{ji} \in D, i = 1 \dots n, j = 1 \dots m$$

is a sample and $c_j \in C$ is the corresponding class. We establish n classifier for each element of the samples, where the $I_k, k = 1, \dots n$ is trained using

$$Y_k = \{x_{1k}, \dots, x_{mk}\}.$$

Let $f_k(y)$ is the probability density function of Y_k. We establish a kernel density estimator $\hat{f}_{hk}(y)$ to approximate $f_k(y)$:

$$\hat{f}_{hk}(y) = \frac{1}{mh}\sum_{i=1}^{m} K\left(\frac{y - y_i}{h}\right),$$

where $y \in Y_k$, h is a smoothing parameter and K is a Gaussian kernel function (with $\mu = 0, \sigma = 1$):

$$K\left(\frac{y - y_i}{h}\right) = \frac{1}{\sqrt{2\pi}} \exp\left(\frac{-(y-y_i)^2}{2h^2}\right).$$

We establish kernel density estimators for each class, from which the membership probability function $P : D \to \mathbb{R}$ can be derived. Thus, we define I_k with the following formula:

$$I_k(x) = \underset{C}{\operatorname{argmax}}\, P(x|C).$$

The final classification for the sample Z by the ensemble O is decided using the following formula:

$$O(Z) = \{C_k | \sum_{i=1}^{m} g_i(C_k) = \max \sum_{i=1}^{m} g_i(C_l)\},$$

$$k, l = 1, \dots, m,$$

where

$$g_i(C_k) = \begin{cases} 1, & I_i = C_k, \\ 0, & otherwise. \end{cases}$$

In our case, the samples are subimages, while the kernel density estimation are based on the pixel intensities.

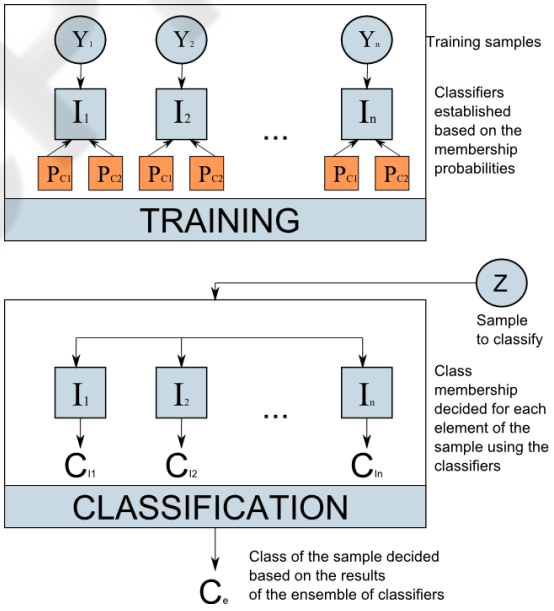

Figure 8: Stages of classification.

In Figure 9 we can see the effect of this classification method applied to the previously shown example output. We can see how a large number of FPs has been removed.

Committee, U. N. S. (2009). *National Screening Programme for Diabetic Retinopathy*. http://www.retinalscreening.nhs.uk/.

Fleming, A. D., Philip, S., and Goatman, K. A. (2006). Automated microaneurysm detection using local contrast normalization and local vessel detection. *IEEE Transactions on Medical Imaging*, 25(9):1223–1232.

Frame, A. J., Undrill, P. E., Cree, M. J., Olson, J. A., McHardy, K. C., Sharp, P. F., and Forrester, J. (May 1998). A comparison of computer based classification methods applied to the detection of microaneurysms in ophthalmic fluorescein angiograms. *Computers in Biology and Medicine*, 28:225238.

Harding, S., Greenwood, R., Aldington, S., Gibson, J., Owens, D., Taylor, R., Kohner, E., Scanlon, P., and Leese, G. (December 2003). Grading and disease management in national screening for diabetic retinopathy in england and wales. *Diabetic Medicine*, 20:965971.

Hejlesen, O., Ege, B., Englemeier, K.-H., Aldington, S., McCanna, L., and Bek, T. (2004). Tosca-imaging developing internet based image processing software for screening and diagnosis of diabetic retinopathy. *MEDINFO 2004*, pages 222–226.

Johnson, N. P. (2004). Advantages to transforming the receiver operating characteristic (roc) curve into likelihood ratio co-ordinates. *Stastics in Medicine*, 23:22572266.

Kirkpatrick, S., Gelatt, C. D., and Vecchi, M. P. (May 13, 1983). Optimization by simulated annealing. *Science*, 220:671–680.

Lazar, I., Hajdu, A., and Quareshi, R. J. (2010). Retinal microaneurysm detection based on intensity profile analysis. *8th International Conference on Applied Informatics*.

Mizutani, A., Muramatsua, C., Hatanakab, Y., Suemoria, S., Haraa, T., and Fujita, H. (2009). Automated microaneurysm detection method based on double-ring filter in retinal fundus images. *Medical Imaging 2009: Computer-Aided Diagnosis, Proceedings of SPIE*, 7260, 7260:1N1 – 1N8.

Niemeijer, M., Staal, J., Abramoff, M. D., Suttorp-Schulten, M. A., and van Ginneken, B. (May 2005). Automatic detection of red lesions in digital color fundus photographs. *IEEE Transactions on Medical Imaging*, 24:584–592.

Niemeijer, M., van Ginneken, B., Cree, M., Mizutani, A., Quellec, G., Sanchez, C., Zhang, B., Hornero, R., Lamard, M., Muramatsu, C., Wu, X., Cazuguel, G., You, J., Mayo, A., Li, Q., Hatanaka, Y., Cochener, B., Roux, C., Karray, F., Garcia, M., Fujita, H., and Abramoff, M. (2010). Retinopathy online challenge: Automatic detection of microaneurysms in digital color fundus photographs. *IEEE Transactions on Medical Imaging*, 29(1):185–195.

Reza, A. M. (2004). Realization of the contrast limited adaptive histogram equalization (clahe) for real-time image enhancement. *The Journal of VLSI Signal Processing*, 38:35–44.

Spencer, T., Olson, J. A., McHardy, K. C., Sharp, P. F., and Forrester, J. V. (May 1996). An image-processing strategy for the segmentation and quantification of microaneurysms in fluorescein angiograms of the ocular fundus. *Computers and Biomedical Research*, 29:284302.

Staal, J., Abramoff, M. D., Niemeijer, M., Viergever, M. A., and van Ginneken, B. (2004). Ridge-based vessel segmentation in color images of the retina. *IEEE Transactions on Medical Imaging*, 23:501 – 509.

Walter, T., Massin, P., Arginay, A., Ordonez, R., Jeulin, C., and Klein, J. C. (2007). Automatic detection of microaneurysms in color fundus images. *Medical Image Analysis*, 11:555–566.

Zuiderveld, K. (1994). Contrast limited adaptive histogram equalization. *Graphics gems*, IV:474–485.